Response to Editor and Reviewer Comments

For clarity, the reviewer's comments are listed below in black italics type, our responses are in black normal type, and changes in the revised version are highlighted in blue.

Editor:

(Q1) *While the authors' revisions have substantially improved the clarity of the manuscript and addressed many of the reviewers' questions and doubts, there remain outstanding concerns about the validity of the chemical modeling used to interpret OFR results. In particular, as referee #3 pointed out in the initial round of reviews, the lack of NO_x dependence in the observed acid yields is a surprising and important result and therefore merits careful substantiation based on modeling of OFR parameters; however, referee #2 points out in this round of re-review that the present modeling provides a confusing set of HO_x and NO_x concentrations for experiments performed with N_2O that seems potentially internally inconsistent. I encourage the authors to provide further detail on the chemical mechanism to referee #2 to verify their simulated HO_x and NO_x concentrations, which will hopefully enable us to proceed toward publication.*

I would also encourage the authors to include more of their analysis of the relative contribution of photolysis e.g., the Figures R1 and R2 (=R4?) prepared for their previous response, and some discussion of the choice of variables and type of modeling that went into producing them in at least the SI of this manuscript, with some pointing to this in the main text; that should satisfactorily address referee #3's re-review request that the response to Q5 be included in the manuscript. It looks like the response to Q6, regarding temperature effects, is already satisfactorily included in the manuscript, so no need to address that comment on referee #3's re-review.

Response: Thank you for your clear guidance and constructive summary of the remaining concerns. Following the suggestion, we have expanded the description and evaluation of the OFR chemical modeling. In the revised Supplement, we have provided the added chemical reactions and rate constants (Table S1), the key model inputs (Table S2), and the modeled •OH, HO_2•, NO, and NO:HO_2• values under each N_2O condition (Table S4). We have also added a comparison between measured and simulated toluene and O_3 concentrations under the N_2O addition experiments (Figure S7), together with the previous O_3 and SO_2 decay evaluation, to support the applicability of the model simulations to our OFR conditions. We have moved the figures comparing the relative contributions of O_3 reactions and 254 nm photolysis with •OH initiated oxidation into the Supplement as Figures S4 and S5, with corresponding discussion in the Supplement and a brief pointer in the main text.

Reviewer #2:

(Q1) *In the revised paper, the authors have provided some key details and clarifications for this study, which I appreciate. However, I still find several inconsistencies in these details, some of which prevent me from well verifying the validity of the key results of this study. The most critical ones are the model predictions about the conditions in their OFR:*

The experimental conditions (O_3 concentration, UV photon flux, residence time etc.) are of the same order of magnitude as Fig. 12(c) in the review paper of Peng and Jimenez (Chem. Soc. Rev., 2020). In the multi-panel figure covering a lot of physical conditions, no condition could result in "high NO" ($NO:HO_2 > 1$), while the authors claimed that $NO:HO_2$ could be up to 10^3.

With such a low initial O_3 concentration, I doubt that OH concentration could be of the order of 10^8-10^9 molecules/cm^3 in the experiments, as very high amounts of NO_x should have been produced from N_2O and lowered OH concentration probably by orders of magnitude relative to conditions without N_2O added.

I am wondering what chemical scheme the authors used for the OFR chemical modeling in this study. If their model may not be able to well characterize the most important parameters of their experiments such as $NO:HO_2$ and OH concentration, all analysis and discussions based on them (organic acid formation pathway, role of UV light etc.) cannot be properly verified. I urge the authors to provide more detail on how the modeling (particularly OFR chemical modeling) was performed. If the key inconsistencies are not resolved, this paper cannot be accepted for publication.

Response: Thank you for your comments and suggestions. We agree with the reviewer that the previous version did not provide sufficient information for readers to independently evaluate the OFR radical simulations, especially under N_2O addition. In the revised manuscript and Supplement, we have expanded the description of the OFR chemical model, the model inputs, and the model evaluation.

Briefly, the model includes toluene oxidation chemistry based on MCM v3.3.1, together with radical chemistry involving O_3 photolysis at 254 nm, $O(^1D)$ reactions with H_2O and N_2O, HO_x/NO_x cycling, and relevant photolysis and kinetic reactions. The kinetic and photolysis parameters were taken from MCM, JPL/NASA recommendations, previous OFR modeling studies, and other evaluated sources (Jenkin et al., 2015; Keller-Rudek et al., 2013; Li et al., 2015). The model was constrained by the measured experimental conditions, including O_3 concentration, RH, temperature, N_2O, and initial toluene concentration. We have added Table S1 to summarize the additional reactions and rate constants used in the model, Table S2 to list the key model input parameters, and Table S4 to report the modeled •OH, HO_2•, NO, and $NO:HO_2$• values under each N_2O condition.

Regarding the concern about the simulated •OH concentration, we agree that N_2O addition can suppress •OH by competing with H_2O for $O(^1D)$ and by enhancing NO_x chemistry. This effect was explicitly included in our model. With increasing N_2O addition, the modeled OH concentration decreased by approximately one order of magnitude, from 2.92×10^9 to 1.80×10^8 molecules cm^{-3} at 20% RH. Thus, the revised simulations do not assume unchanged •OH exposure after N_2O addition; rather, the reported •OH concentrations are model outputs after accounting for N_2O-induced •OH suppression. To evaluate whether these modeled •OH levels are reasonable, we compared the model results with independent experimental constraints. As shown in Fig. S3, the model reproduced the observed O_3 and SO_2 decay, supporting its ability to capture the primary oxidant production and loss processes. Additionally, we further added a comparison between measured and simulated toluene decay under the experimental conditions used in this study. The simulated and measured toluene decay showed reasonable agreement (Figure S7), indicating that the model captures the effective oxidative conditions experienced by toluene in the OFR. Therefore, although the initial O_3 concentration in our experiments was lower than that in some previous OFR254-iN_2O studies (Lambe et al., 2017; Peng

and Jimenez, 2020), the agreement between measured precursor decay and model simulations supports the modeled •OH concentration range of 10^8–10^9 molecules cm^{-3}.

Regarding the NO:HO_2• ratio, we agree that Fig. 12(c) of Peng and Jimenez (2020) provides a useful reference for evaluating radical regimes in OFR254-iN_2O systems. As listed in Table S2, our experimental conditions are most comparable to Cases MM and HM, for which high NO conditions are predicted when the N_2O mixing ratio exceeds approximately 2%. Because the N_2O mixing ratios used in our study ranged from 0 to 10% (0, 1%, 2%, 4%, 6%, 8%, and 10%), Fig. 12(c) does not exclude the occurrence of high-NO conditions under our experimental conditions, particularly at higher N_2O levels. It should be noted that the "good", "risky", and "bad" classifications shown in Fig. 12(c) refer to the atmospheric relevance of OFR conditions rather than indicating the magnitude of NO:HO_2• ratio (or $r(RO_2• + NO)/r(RO_2• + HO_2•)$ ratio). Therefore, this figure cannot be used to directly infer the absolute NO:HO_2• ratios under our specific experimental conditions. In contrast, our model results, now summarized in Table S4, explicitly show that the NO:HO_2• ratio increased systematically with increasing N_2O addition. The feasibility of elevated NO:HO_2• ratios in OFR254-iN_2O systems is further supported by another related study conducted by their collaborators (Lambe et al., 2017), which employed the same method of OFR254-iN_2O to achieve high NO conditions as well. Their simulations showed that NO:HO_2• ratio depends on H_2O, O_3, UV intensity, and precursor (e.g., VOCs) conditions (Figs. S2-S7 in Lambe et al. (2017)), and can reach values as high as 10^5. For example, as shown in Fig. S7 of Lambe et al. (2017), under conditions of $I_{254} = 1.8 \times 10^{15}$ photons cm^{-2} s^{-1}, [H_2O] = 0.07%, [α-pinene] = 15 ppb, [O_3] = 5 ppm, and [N_2O] = 3.2%, the modelled NO concentration and NO:HO_2• ratio were ~4 ppbv and ~100, respectively. In our study, under comparable OFR254-iN_2O conditions (I_{254} = ~2.9×10^{15} photons cm^{-2} s^{-1}, [H_2O] = 0.63% (T = 298 K; RH = 20%), [toluene] = 94 ppb, [O_3] = 1.58 ppm, and [N_2O]= 4%), the modeled NO concentration and NO:HO_2• ratio were 11.36 ppbv and 55.3, respectively. These comparisons support the feasibility of elevated NO:HO_2• ratios under our OFR254-iN_2O conditions and indicate that a NO:HO_2• ratio approaching 10^3 under the highest N_2O condition (10%) is plausible. Moreover, consistent with our simulations, Lambe et al. (2017) also found that •OH exposure decreased by approximately one order of magnitude, from ~10^{11} to ~10^{10} molecules cm^{-3} s, corresponding to an average •OH concentration decrease from the 10^9 to 10^8 molecules cm^{-3} level. We have added further details on model simulation and validation in the revised manuscript and Supplement to support the reliability of the modeled •OH, HO_2•, and NO concentrations.

Page 8: "The detailed chemical reactions added to the model and their corresponding rate constants are provided in Table S1. The initial concentrations of toluene, O_3, water vapor, and N_2O, together with temperature, residence time, and $J(O_3 \rightarrow O(^1D))$, were set according to the experimental conditions summarized in Table S2."

Page 12: "As shown in Figure 3, molar yields of formic acid and acetic acid were not significantly affected by NO concentration at either 20% or 70% RH. Even at the highest NO level (~29 ppbv at 20% RH), where the modeled NO:HO_2• ratio approached 1000 (Table S4), substantial production of organic acids (~40% for formic acid and ~20% for acetic acid at 20% RH) was still observed."

Page 12: "Moreover, the persistence of high organic acid yields despite the substantial decrease in simulated •OH concentration from 2.92×10^9 to 1.80×10^8 molecules cm^{-3} and the corresponding decrease in toluene consumption from ~60 ppbv to ~25 ppbv with increasing N_2O addition (Table S4 and Figure S7) further supports this conclusion and suggests that NO may even facilitate organic acid production through enhanced alkoxy radical formation and subsequent fragmentation."

Table S1. Reactions added to the MCM model and their corresponding rate constants.

No.	Reactions	Rate (cm^3 $molecule^{-1}$ s^{-1} or s^{-1})
1	$N_2O + O^1D \rightarrow NO+NO$	7.6×10^{-11}
2	$O^1D + CO_2 \rightarrow O + CO_2$	$7.5\times10^{-11}\times e^{115/T}$
3	$O^1D + H_2 \rightarrow OH + H$	1.2×10^{-10}
4	$O^1D + N_2 + M \rightarrow N_2O$	$2.8\times10^{-36}\times(300/T)^{0.88}$
5	$O + OH \rightarrow O_2 + H$	$2.4\times10^{-11}\times e^{110/T}$
6	$O + HO_2 \rightarrow O_2 + OH$	$3.0\times10^{-11}\times e^{200/T}$
7	$O + H_2O_2 \rightarrow HO_2 + OH$	$1.4\times10^{-12}\times e^{-2000/T}$
8	$O + HO_2NO_2 \rightarrow$ products	$7.8\times10^{-11}\times e^{-3400/T}$
9	$H + O_3 \rightarrow OH + O_2$	$1.4\times10^{-10}\times e^{-470/T}$
10	$H + HO_2 \rightarrow OH + OH$	7.2×10^{-11}
11	$H + HO_2 \rightarrow O + H_2O$	1.6×10^{-12}
12	$H + HO_2 \rightarrow O_2 + H_2$	6.9×10^{-12}
13	$H + NO_2 \rightarrow NO + OH$	$4.0\times10^{-10}\times e^{-340/T}$
14	$NO_3 + NO_3 \rightarrow O_2 + NO_2 + NO_2$	$8.5\times10^{-13}\times e^{-2450/T}$
15	$N_2O_5 + H_2O \rightarrow HNO_3 + HNO_3$	2.0×10^{-21}
16	$HCHO + HO_2 \rightarrow HOCH_2O_2$	$9.7\times10^{-15}\times e^{625/T}$
17	$HOCH_2O_2 \rightarrow HO_2 + HCHO$	$2.4\times10^{12}\times e^{-7000/T}$
18	$HOCH_2O_2 + HO_2 \rightarrow HOCH_2O_2H$	$5.6\times10^{-15}\times e^{2300/T}\times0.5$
19	$HOCH_2O_2 + HO_2 \rightarrow HCOOH$	$5.6\times10^{-15}\times e^{2300/T}\times0.3$
20	$HOCH_2O_2 + HO_2 \rightarrow OH + HOCH_2O$	$5.6\times10^{-15}\times e^{2300/T}\times0.2$
21	$HOCH_2O_2 + NO \rightarrow NO_2 + HOCH_2O$	5.6×10^{-12}
22	$HOCH_2O_2 + HOCH_2O_2 \rightarrow HCOOH + HOCH_2OH$	$5.7\times10^{-14}\times e^{750/T}$
23	$HOCH_2O_2 + HOCH_2O_2 \rightarrow HOCH_2O + HOCH_2O$	5.5×10^{-12}
24	$HOCH_2O_2H + OH \rightarrow HOCH_2O_2$	$3.1\times10^{-11}\times0.12$
25	$HOCH_2O_2H + OH \rightarrow HCOOH + OH$	$3.1\times10^{-11}\times0.88$
26	$HOCH_2O \rightarrow HCOOH + HO_2$	5×10^{14}
27	$HOCH_2OH + OH \rightarrow HCOOH + HO_2$	1.1×10^{-11}
28	$CH_3CHO \rightarrow VINOH$	$J_{13}\times1.5 + 1.17\times10^{-19}\times T^{1.2}\times e^{-279.8/T}\times$[Acids][a]
29	$VINOH \rightarrow CH_3CHO$	$4.67\times10^{-26}\times T^{3.3}\times e^{2269/T}\times$[Acids][a]
30	$VINOH + OH \rightarrow HCOOH + OH + HCHO$	3.8×10^{-11}
31	$VINOH+OH\rightarrow HOCH_2CHO + HO_2$	2.4×10^{-11}
32	$VINOH + OH \rightarrow VINOHOHO_2$	5.2×10^{-12}
33	$VINOHOHO_2 + NO \rightarrow HCOOH + HCHO + NO_2$	1.0×10^{-11}
34	$OH + HCHO \rightarrow HCOOH + HO_2$	2.0×10^{-13}
35	$CH_3O_2 + OH \rightarrow CH_2OOA$	2.8×10^{-10}
36	$CH_2OOA \rightarrow CH_2OO$	KDEC×0.37[b]
37	$CH_2OOA \rightarrow CO$	KDEC×0.50
38	$CH_2OOA \rightarrow HO_2 + CO + OH$	KDEC×0.13
39	$CH_2OO+CO \rightarrow HCHO$	1.2×10^{-15}
40	$CH_2OO + NO \rightarrow HCHO + NO_2$	1.0×10^{-14}
41	$CH_2OO + NO_2 \rightarrow HCHO + NO_3$	1.0×10^{-15}
42	$CH_2OO \rightarrow HCHO + H_2O_2$	$6.0\times10^{-18}\times H_2O$
43	$CH_2OO \rightarrow HCOOH$	$1.0\times10^{-18}\times H_2O$
44	$HCOOH + OH \rightarrow HO_2$	4.5×10^{-13}

[a]The model considers the combined concentrations of formic acid and acetic acid; J_{13} is the photolysis rate of acetaldehyde. [b]KDEC = 1×10^6.

Table S2. Key input parameters used in the box model simulations.

No.	Parameters	Values
1	RH	20% or 70%
2	T	298 K
3	Toluene	94 ppbv
4	Ozone	1580 ppbv
5	N_2O	(0, 0.01, 0.02, 0.04, 0.06, 0.08, and 0.1) × M[a]
6	$J_{O_3 \rightarrow O^1D}$	3.01×10^{-2} s^{-1}
7	Residence time	3.9, 15.8, 27.5, 39.3, 51.0, and 60.0 s

[a]Total number density of gas molecules.

Table S4. The modeled concentrations of •OH, HO_2•, and NO, as well as the ratio of NO:HO_2• under different experimental conditions with the addition of N_2O.

No.	Initial N_2O (%)	•OH (molecules cm^{-3})		HO_2• (molecules cm^{-3})		NO (ppbv)		NO:HO_2•	
		20%RH	70%RH	20%RH	70%RH	20%RH	70%RH	20%RH	70%RH
0	0%	2.92×10^{9}	1.90×10^{10}	9.45×10^{9}	1.19×10^{10}	0.00	0.0	0.00	0.0
1	1%	1.97×10^{9}	1.37×10^{10}	1.67×10^{10}	1.72×10^{10}	1.82	0.6	2.7	0.9
2	2%	1.40×10^{9}	9.51×10^{9}	1.38×10^{10}	2.42×10^{10}	4.78	2.1	8.5	2.2
3	4%	6.88×10^{8}	4.59×10^{9}	5.05×10^{9}	1.90×10^{10}	11.36	6.6	55.3	8.6
4	6%	3.95×10^{8}	2.40×10^{9}	2.21×10^{9}	1.04×10^{10}	17.66	12.0	196.4	28.4
5	8%	2.56×10^{8}	1.41×10^{9}	1.18×10^{9}	5.71×10^{9}	23.4	17.5	489.4	75.3
6	10%	1.80×10^{8}	9.18×10^{8}	7.09×10^{8}	3.42×10^{9}	28.7	22.7	995.1	163.1

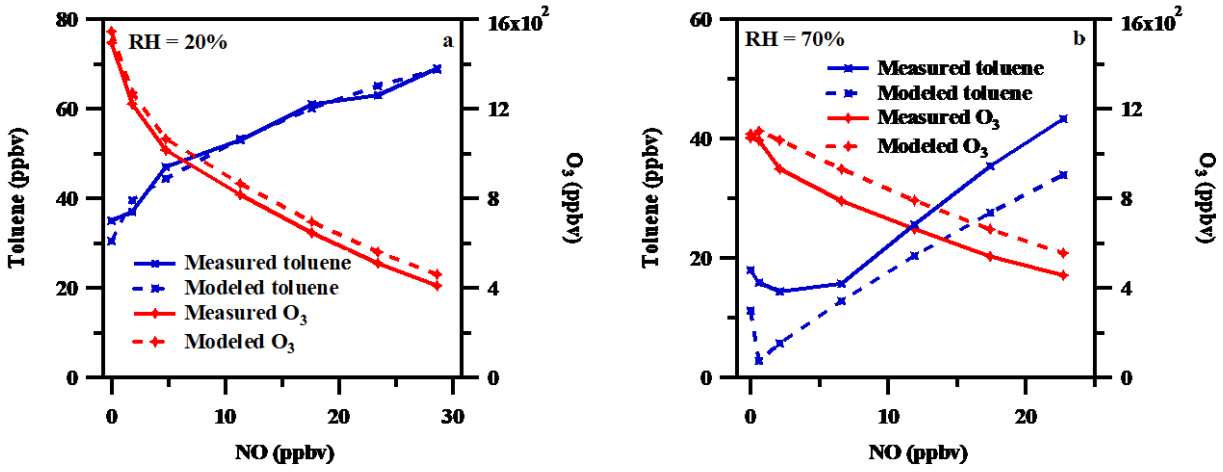

Figure S7. Comparison of observed and simulated toluene and O_3 concentrations as a function of NO concentration. (a) 20% RH; (b) 70% RH.

References:

Jenkin, M. E., Young, J. C., and Rickard, A. R.: The MCM v3.3.1 degradation scheme for isoprene, Atmos. Chem. Phys., 15, 11433–11459, https://doi.org/10.5194/acp-15-11433-2015, 2015.

Jenkin, M. E., Valorso, R., Aumont, B., and Rickard, A. R.: Estimation of rate coefficients and branching ratios for reactions of organic peroxy radicals for use in automated mechanism construction, Atmos. Chem. Phys., 19, 7691–7717, https://doi.org/10.5194/acp-19-7691-2019,

2019.
Keller-Rudek, H., Moortgat, G. K., Sander, R., and Sörensen, R.: The MPI-Mainz UV/VIS Spectral Atlas of Gaseous Molecules of Atmospheric Interest, Earth Syst. Sci. Data, 5, 365–373, https://doi.org/10.5194/essd-5-365-2013, 2013.
Lambe, A., Massoli, P., Zhang, X., Canagaratna, M., Nowak, J., Daube, C., Yan, C., Nie, W., Onasch, T., Jayne, J., Kolb, C., Davidovits, P., Worsnop, D., and Brune, W.: Controlled nitric oxide production via $O(^1D) + N_2O$ reactions for use in oxidation flow reactor studies, Atmos. Meas. Tech., 10, 2283–2298, https://doi.org/10.5194/amt-10-2283-2017, 2017.
Li, R., Palm, B. B., Ortega, A. M., Hlywiak, J., Hu, W., Peng, Z., Day, D. A., Knote, C., Brune, W. H., De Gouw, J. A., and Jimenez, J. L.: Modeling the Radical Chemistry in an Oxidation Flow Reactor: Radical Formation and Recycling, Sensitivities, and the OH Exposure Estimation Equation, J. Phys. Chem. A, 119, 4418–4432, https://doi.org/10.1021/jp509534k, 2015.
Peng, Z. and Jimenez, J. L.: Radical chemistry in oxidation flow reactors for atmospheric chemistry research, Chem. Soc. Rev., 49, 2570–2616, https://doi.org/10.1039/C9CS00766K, 2020.
Peng, Z., Lee-Taylor, J., Orlando, J. J., Tyndall, G. S., and Jimenez, J. L.: Organic peroxy radical chemistry in oxidation flow reactors and environmental chambers and their atmospheric relevance, Atmos. Chem. Phys., 19, 813–834, https://doi.org/10.5194/acp-19-813-2019, 2019.

Reviewer #3:

The authors have provided detailed responses, but two issues remain unresolved. Please address each point below before final acceptance.

***(Q1)** Please provide supporting references for the newly added statement in lines 287-290: "NO primarily reacts with RO_2 to form alkoxy radicals (RO•), ….*

Response: We have added supporting citations in the revised manuscript.

Page 11-12: "NO primarily reacts with RO_2• to form alkoxy radicals (RO•) (Jenkin et al., 2019; Peng et al., 2019), which can divert the traditional organic acid formation pathway toward carbonyl products."

***(Q2)** I could not find any indications, modifications, or supplements in the main text corresponding to Q5 and Q6 from the previous round of review. These should be reflected in the manuscript.*

Response: In the revised manuscript, we have revised Section 2.1 to state that the internal OFR temperature was maintained at 298 ± 1 K under all experimental conditions. We have also revised Section 3.1.2 and the Supplement to clarify how •OH, HO_2•, NO, and NO:HO_2• were simulated under N_2O addition.

Page 5: "The reactor temperature was maintained at 298 ± 1 K by a continuously circulating water jacket. No systematic temperature increase was observed with increasing lamp number or •OH exposure, even when all eight lamps were illuminated."

Page 12: "Moreover, the persistence of high organic acid yields despite the substantial decrease in simulated •OH concentration from 2.92×10^9 to 1.80×10^8 molecules cm^{-3} and the corresponding decrease in toluene consumption from ~60 ppbv to ~25 ppbv with increasing N_2O addition (Table S4 and Figure S7) further supports this conclusion and suggests that NO may even facilitate organic acid production through enhanced alkoxy radical formation and subsequent fragmentation."